AN INVESTIGATION OF FLOW SEPARATION IN AN OVEREXPANDED SUPERSONIC NOZZLE

Thesis by

John Dill McKenney

In Partial Fulfillment of the Requirements

for the Degree of

Aeronautical Engineer

California Institute of Technology

Pasadena, California

1949

ACKNOWLEDGMENTS

The author wishes to express his sincere appreciation for the advice and assistance freely given by Mr. Allen E. Puckett and Dr. Martin Summerfield and Mr. Nathaniel Van de Verg of the Jet Propulsion Laboratory. The author is also indebted to Mr. Marvin Jessey for valuable comments on the shadowgraph technique used.

ABSTRACT

An apparatus for the investigation of flow separation in a supersonic nozzle has been designed and constructed. Nozzle wall pressure distributions and shadowgraphs showing the associated shock wave configuration have been obtained for a range of different stagnation pressures and constant exit pressure.

The pressure ratios were such that the theoretical nozzle exit pressure, without separation, was always less than atmospheric pressure. With the nozzle contour and pressure ratios investigated it is found that separation of flow from the nozzle walls always occurs. The separation is accompanied by a weak oblique shock wave of such strength that the flow deflection through it is approximately constant, independent of the location of the point of separation within the nozzle. The pressure adjustment from nozzle to exit does not occur through a normal shock wave.

At pressure ratios below a certain value a definite asymmetry of flow appears in which the detached jet deflects away from the nozzle symmetry axis. At higher pressure ratios, the flow becomes stable with separation occurring at the same distance from the nozzle throat on both upper and lower walls.

TABLE OF CONTENTS

I. INTRODUCTION

The character of flow in a De Laval nozzle is dependent on the relative magnitudes of the pressure at the nozzle exit P_e and the pressure P_a of the region into which the nozzle exhausts. When P_e equals P_a, the flow leaves the nozzle exit smoothly without shock or expansion waves. When P_e is greater than P_a, the adjustment occurs through expansion waves. When P_e is less than P_a, several different flow configurations are possible. An oblique shock wave provides the pressure increase necessary when P_e is only slightly less than P_a. As P_a decreases from that pressure corresponding to oblique shock waves at the nozzle exit, separation occurs. It is this last pressure condition and the associated separation which is the subject of this investigation.

One of the first investigations of this problem was made by Stodola, (Ref. 1), in the development of steam turbine nozzles. Eggink, (Ref. 2), obtained schlieren photographs of flow separation in a divergent section in his work on the pressure recovery in supersonic wind tunnel diffuser. Weise, (Ref. 3), also obtained schlieren photographs of separation in nozzles when concerned with the effect of separation on the performance of supersonic compressors.

The direct background for this investigation is the research which has been conducted at the California Institute of Technology Jet Propulsion Laboratory and which was described in a paper presented by Summerfield at the 1948 meeting of the Institute of Fluid Mechanics and Heat Transfer, (Ref. 4). The increases in performance caused by flow separation in the nozzle of a rocket motor operating at

an altitude less than that for which it was designed are discussed by Swan, (Ref. 5). An experimental investigation of separation in the nozzle of a rocket motor has been made by Foster, (Ref. 6).

In the investigation by Foster, the behavior of the flow separation is studied by considering the measured variations in nozzle wall static pressures. Since it was desirable to have a more direct means of investigating separation, the transparent nozzle described in this thesis was designed and constructed. With this apparatus it is possible to obtain shadowgraphs showing the separation.

The objective, then, of this investigation is to determine, for a given nozzle geometry, if and in what manner separation occurs when the nozzle is operating at a pressure ratio less than the pressure ratio corresponding to oblique shock waves at the exit of the nozzle. Further investigations would be concerned with the effect of variations of additional parameters such as nozzle geometry.

II. EXPERIMENTAL APPARATUS

The experimental apparatus consists of a small two-dimensional nozzle, a high pressure nitrogen supply system and a spark shadowgraph.

The nozzle consists of two brass nozzle blocks clamped between parallel glass windows. The contour of the nozzle blocks was arbitrarily selected as one often used in rocket nozzles. The straight convergent and divergent portions are joined by a circular arc at the nozzle throat. The two nozzle blocks were machined while doweled together to insure similarity of the contoured faces. Ten static pressure orifices are spaced along each polished nozzle block face. The thickness of the nozzle blocks and the spacing of the parallel glass sides is .370 inches since no gasket is used between the blocks and the glass. The vertical spacing of the blocks forms a .20 inch throat and 1.60 inch exit so that the ratio of exit to throat area is eight to one. The nozzle blocks are positioned with respect to each other by dowel pins which pass through the blocks and the side cover plates which clamp the whole assembly together. The glass windows are ordinary plate glass .75 inches thick. It is apparently of satisfactory quality for use with the shadowgraph technique. The nozzle is shown in Figs. 1-3.

The use of dry hitrogen supplied from a bank of ten standard high pressure bottles provides a convenient range of pressures. Dry nitrogen is used for several reasons. It is dry enough so that the occurrence of condensation shock waves is eliminated. The ratio of specific heats for

nitrogen is very nearly equal to that for air, for which convenient oblique shock and flow tables are available. Dry nitrogen is also easily available and is relatively inexpensive.

A manifold connects the ten bottles to a master valve. From this valve the flow goes to the pressure regulating valve. A standard GROVE regulating valve with a pilot loader reduces the pressure from that in the bottles, initially 2,200 psi, to the desired nozzle operating pressure. A tubular settling section connects the regulator valve to the nozzle. The low flow velocity in this settling section allows the stagnation pressure to be measured directly by a 0 to 300 psi bourdon tube type gage. No provision is made for control of the nitrogen temperature which will drop during a test run. This decreasing temperature will cause an increasing mass flow rate for a given stagnation pressure which is of importance only with respect to the amount of nitrogen expended during a test run. The effects of the variations of the physical properties of the gas with the changes in temperature are assumed negligible. The supply of nitrogen is adequate for approximately thirty test runs, each of such duration that the manometer bank comes to equilibrium and a shadowgraph exposure is made. The system is shown schematically in Fig. 4; Fig. 5 is a general view of the test apparatus.

The shadowgraph equipment consists of a high voltage spark power supply, a spark gap, a photographic plate holder for the nozzle and arrangements for preventing stray light from entering the system. The power supply and spark gap are similar to those described in NAVORD Rep. 980, (Ref. 7), however, no precise spark timing circuits are

employed. The spark power supply is a 0.25 mfd condenser which can be charged to any voltage up to twenty kilovolts, then discharged through a light producing spark gap when two gas-filled thyratron tubes are triggered. The resulting spark is of approximately two microseconds duration and very intense. The spark gap is so designed that the light passes through a hole in one of the electrodes forming effectively a point source. The spark gap is mounted in the front of the power supply case. A tube approximately three feet long with internal baffles to cut reflection is mounted between the spark gap and the nozzle. Light from the gap which is placed 40 inches from the nozzle passes through the glass nozzle windows and impinges directly on a 4 by 5 inch Graflex plate holder for the film mounted directly behind the nozzle. The film is approximately 2 inches from the nozzle centerline. Light is prevented from entering the open end of the nozzle by a box containing three offset light baffles.

Static wall pressures are recorded photographically from a multiple tube mercury manometer.

III. TESTING PROCEDURE

The necessity of conserving the nitrogren supply demands individual tests of short duration. All runs were made at constant stagnation pressure as controlled by the regulator valve. An approximate setting of the regulator pilot loader is made and the gate valve on the supply manifold is opened full. Final adjustment of the stagnation pressure is made and as soon as the manometer bank reaches equilibrium, it is photographed, a shadowgraph exposure is made and the supply valve shut as soon as possible.

For check runs to be certain everything was operating properly, exposures were made on Eastman Process Extra printing paper. The use of this paper provided a rapid means of checking the spark behavior since it can be developed quickly. For best results, the exposure is made directly on Eastman Process Panchromatic cut film from which enlargements can be made.

The only adjustments of the shadowgraph apparatus necessary are the spark voltage for proper exposure density and the positioning of the gap with respect to the nozzle. Since there is a small amount of parallax, the nozzle and gap are so aligned that the gap is on a line from approximately the middle of one of the nozzle block faces and perpendicular to the glass windows.

IV. EXPERIMENTAL RESULTS

The primary variable in this investigation is the pressure in the settling section which precedes the nozzle. Since the ratio of the settling section cross sectional area to that of the nozzle throat is 112 to 1, the pressure measured there can be assumed to be equal to the stagnation pressure P_o. The stagnation pressure P_o was varied from 174 to 294 psia in increments of 10 psia. Since the flow is separated from the wall for all pressures investigated, the pressure at the static orifice nearest to the exit is assumed to be equal to the pressure of the region into which the nozzle exhausts. This back pressure P_e was not varied and was constant at 13.1 psia. The pressure ratios P_o/P_e investigated, then, were from $P_o/P_e = 13.3$ to $P_o/P_e = 22.4$.

For comparison the pressure ratio and Mach number at the exit have been computed for the given nozzle geometry. The theoretical pressure ratio P_o/P_e is 100 for isentropic flow to the exit, while the exit Mach number would be 3.68.

a. Pressure measurements

Static pressure distributions along the nozzle walls are presented as functions of the nozzle area ratios. The area ratio is assumed to be the ratio of the plane cross sectional area of the nozzle at the point of interest to the cross sectional area of the throat. The area ratio is geometric, no correction for boundary layer thickness being made.

The variation of $\frac{P}{P_o}$, where P is the static wall pressure and P_o is the stagnation pressure, with area ratio is shown in Fig. 6.

Curves corresponding to several different stagnation pressures are plotted. Also included is a plot of the pressure ratio as a function of the area ratio as determined by the assumption of one-dimensional, isentropic, frictionless flow.

The variation of $\frac{P}{P_e}$ with area ratio is shown in Fig. 7. This plot illustrates the rapid rise in static wall pressures associated with the flow separation. It must be remembered, however, that pressure measurements in the immediate vicinity of the intersection of a shock wave and a wall are of questionable value because of shock wave oscillations and pressure disturbances transmitted upstream through the subsonic portion of the boundary layer.

b. Shadowgraph results

Several typical shadowgraphs taken at different pressure ratios are shown in Fig. 8-11. The spark gap is in the plane of the lower nozzle block face so that the reflection of light from the polished upper nozzle block surface causes the light streak apparently parallel to the upper wall. The point of separation is well defined as are the jet boundaries and the oblique shock waves. The complicated flow pattern downstream of the oblique shock waves intersection is the result of interactions with the boundary layer also present on the glass windows.

From a series of these shadowgraphs the points of separation can be directly determined. From these measurements the ratio of the nozzle cross sectional area at the point of separation to the nozzle throat area can be computed. Fig. 12 is a plot of the

variation of this separation area ratio As/A* with the nozzle pressure ratio $\frac{P_o}{P_e}$. The distortion effects of parallax cause errors of second order in the measurement directly from the shadowgraphs and are therefore neglected. There are small oscillations of the shock structure and the separation point apparent from the scatter of the data presented in Fig. 12. Since the shadowgraph exposures are of such short duration, the flow appears stationary.

The shadowgraphs shown in Fig. 13 and 14 illustrate an interesting flow instability which was present when operating at low stagnation pressures. When the pressure ratio $\frac{P_o}{P_e}$ was less than 12 this asymmetric separation was observed in which the flow separation occurred at different distances from the throat on the upper and lower nozzle walls. The flow even reattaches to the nozzle wall after separation.

V. DISCUSSION OF RESULTS

Swan, (Ref. 5), describes a method by which the behavior of the separation point in a rocket nozzle can be approximately predicted. This hypothesis is based on the assumption of the existence of a separation producing oblique shock wave within the nozzle of such strength that the flow deflection through it remains constant, independent of the position in the nozzle. With this assumption, a given exit pressure and one-dimensional nozzle theory, a relationship between the location of the separation point and the stagnation pressure is defined. For comparison, a family of curves corresponding to different values of this flow deflection have been plotted in Fig. 15. The calculations are shown in the Appendix. It is interesting to note that the 14 degree deflection curve which best agrees with the experimental results is nearly the same deflection as that which agrees best with tests of actual rocket nozzles as shown in Ref. 6.

Fig. 16 is a plot of the pressure ratio P_1/P_e as a function of the nozzle operating pressure ratio P_o/P_e where P_1 is the nozzle wall pressure at the point of flow separation. The pressure at separation is determined from the envelope of the pressure distribution curves in Fig. 6. The pressure is that corresponding to the separation area ratio as determined from shadowgraphs. From this curve we see that the wall pressure ratio at separation is very nearly constant.

Since the nozzle back pressure, or P_e, is constant and the separation pressure is constant as shown by Fig. 16, the possibility

of a simple relation between them is suggested. A further series of tests in which the nozzle back pressure is varied should provide valuable additional information.

VI. CONCLUSIONS

For the particular nozzle investigated it has been found that separation always occurs for a certain range of nozzle pressure ratios. The separation is apparently unstable when the nozzle is operating at a pressure ratio less than 12. At pressure ratios greater than 12 the separation occurs at the same distance from the nozzle throat on both upper and lower nozzle walls.

The separation point moves in the direction of the nozzle exit in a definite manner as the nozzle pressure ratio is increased. It has been found that the location of the point of separation can be predicted by assuming that the separation occurs when the static wall pressure has dropped to a certain constant fraction of the nozzle exit, or atmospheric, pressure.

One should be cautious in applying these results to other problems since this investigation was made with only one primary variable, the nozzle pressure ratio. The effect of other parameters on the behavior of the separation is not known.

REFERENCES

1. Stodola, Aurel, Steam and Gas Turbines, McGraw-Hill, New York, 1927.

2. Eggink, H., "Flow Structure and Pressure Recovery in Supersonic Tunnels", Z.W.B. Forschungsbancht #1756.

3. Weise, A., "The Separation of Flow Due to Compressibility Shock", Technische Berichte Bard 10, Heft 2, 1943.

4. Martin Summerfield, Charles R. Foster, Walter C. Swan, "Flow Separation in Overexpanded Supersonic Exhaust Nozzles", presented at meeting of Institute of Fluid Mechanics and Heat Transfer, Los Angeles, June 22, 1948.

5. Swan, Walter C., "The Influence of Nozzle Design on the Flight Performance of Rocket Vehicles, With an Analysis of the Results of Jet Separation", M. E. Thesis, C.I.T., 1948.

6. Foster, Charles R., Report on the results of tests of overexpended rocket nozzles not yet published. Jet Propulsion Laboratory, C.I.T.

7. Marlow, Nieswanger, "Development of the Spark Shadowgraph", U.S.N. Ordnance Test Station Report, NAVORD #980, Nov. 1947.

FIG. 1 NOZZLE (front cover plate and glass removed)

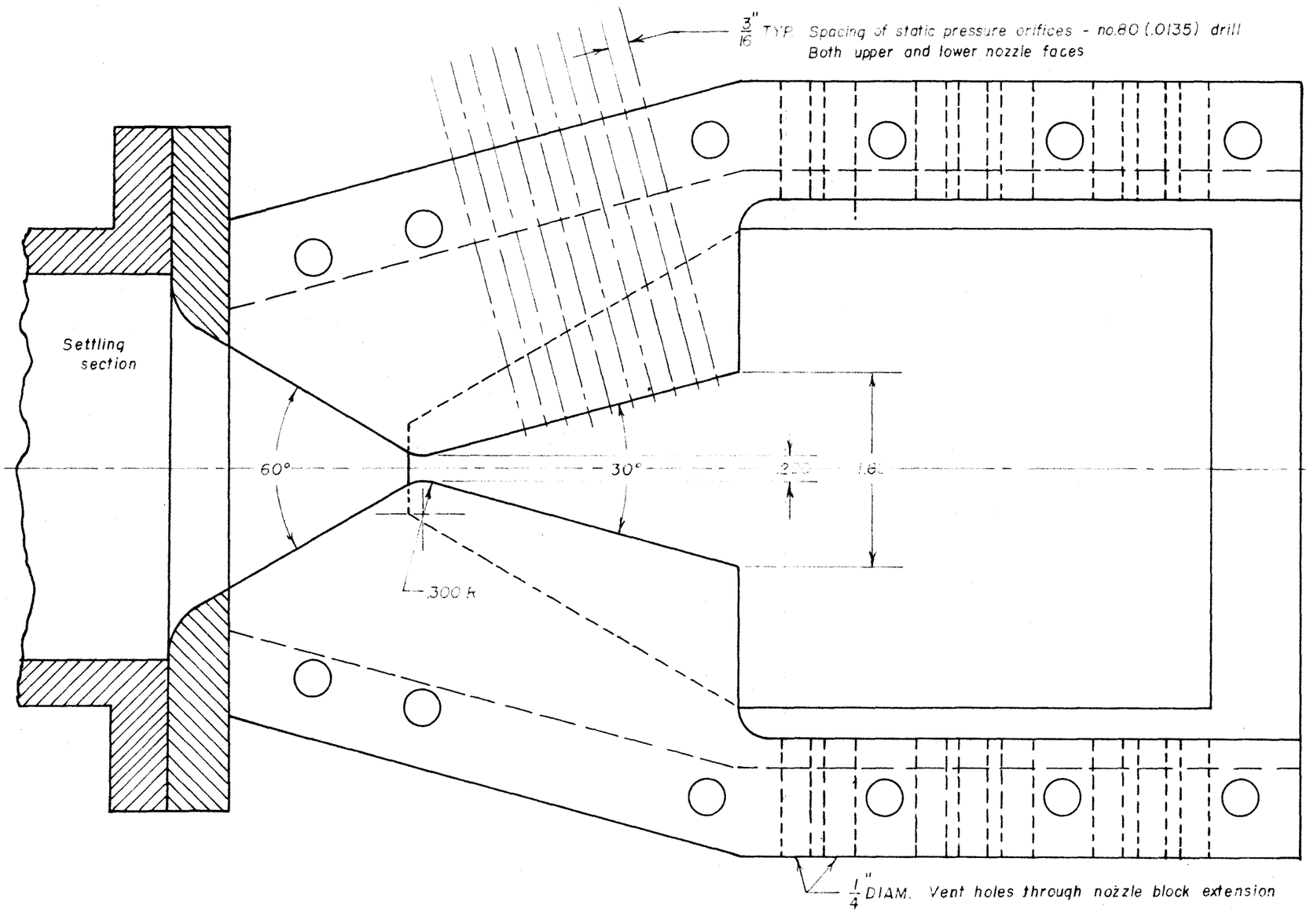

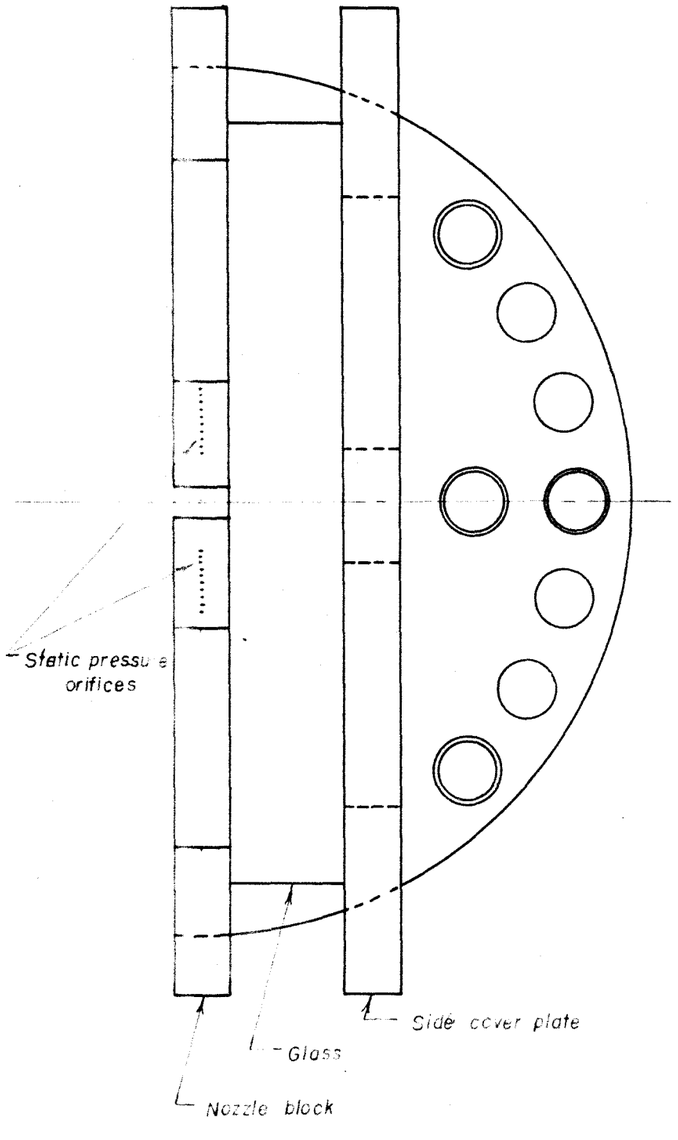

full size

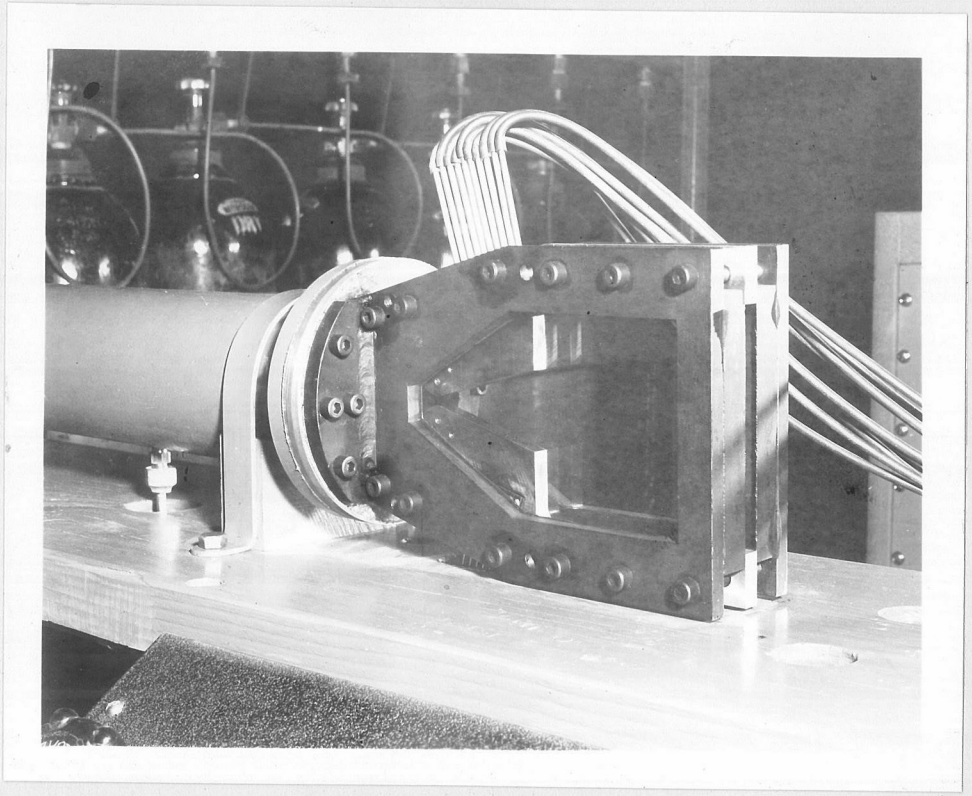

Fig. 2

View of nozzle

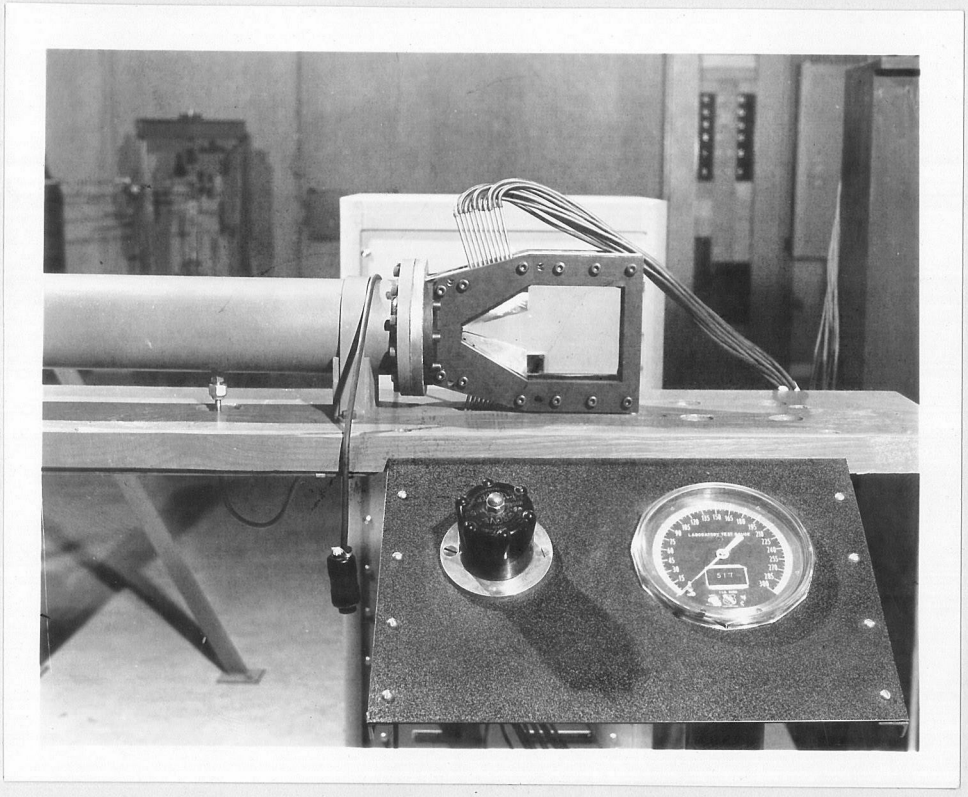

Fig. 3

View of nozzle

FIG. 4 NITROGEN SUPPLY SYSTEM

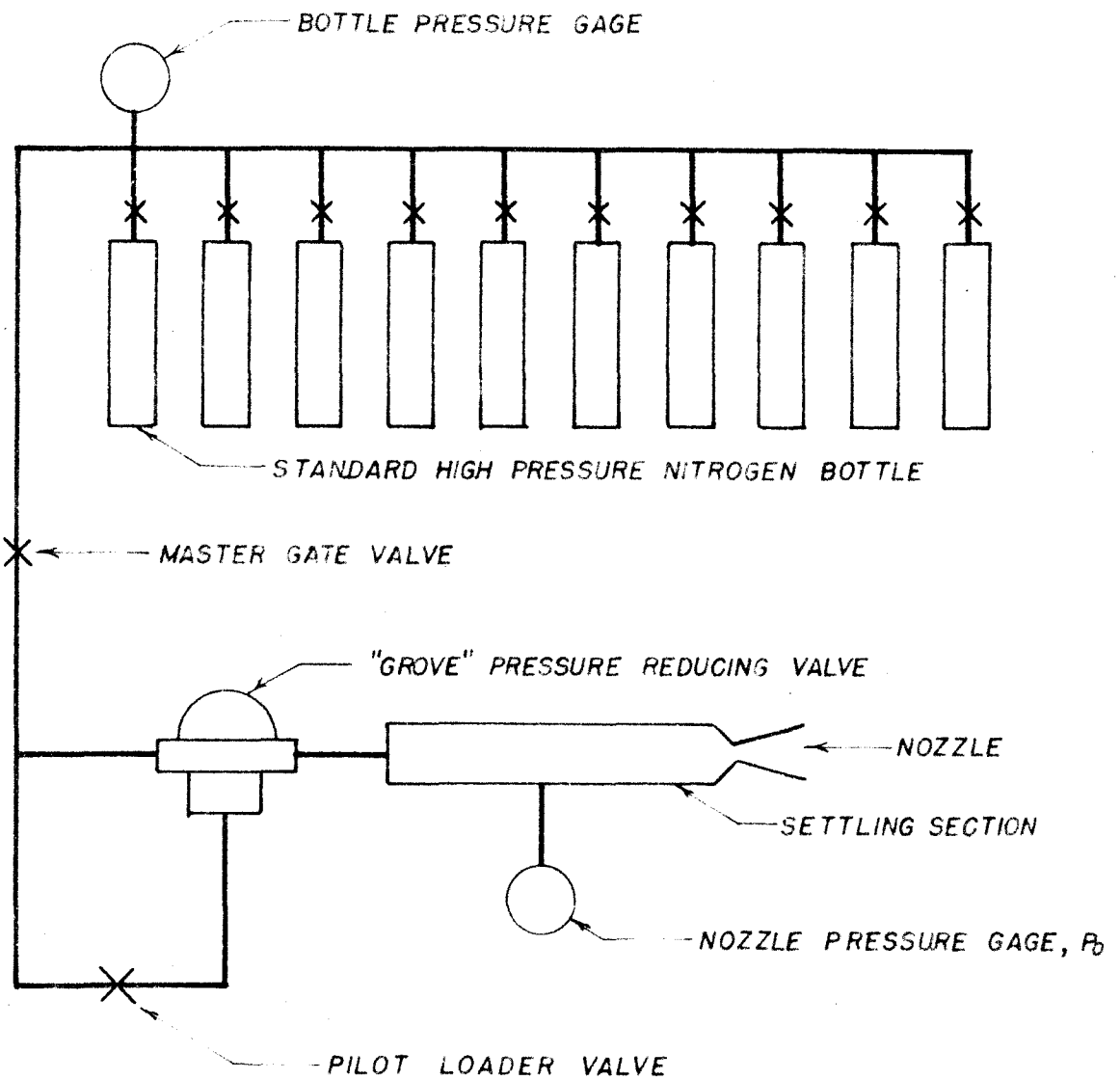

Fig. 5

General view of test apparatus

FIG. 6 PRESSURE DISTRIBUTIONS

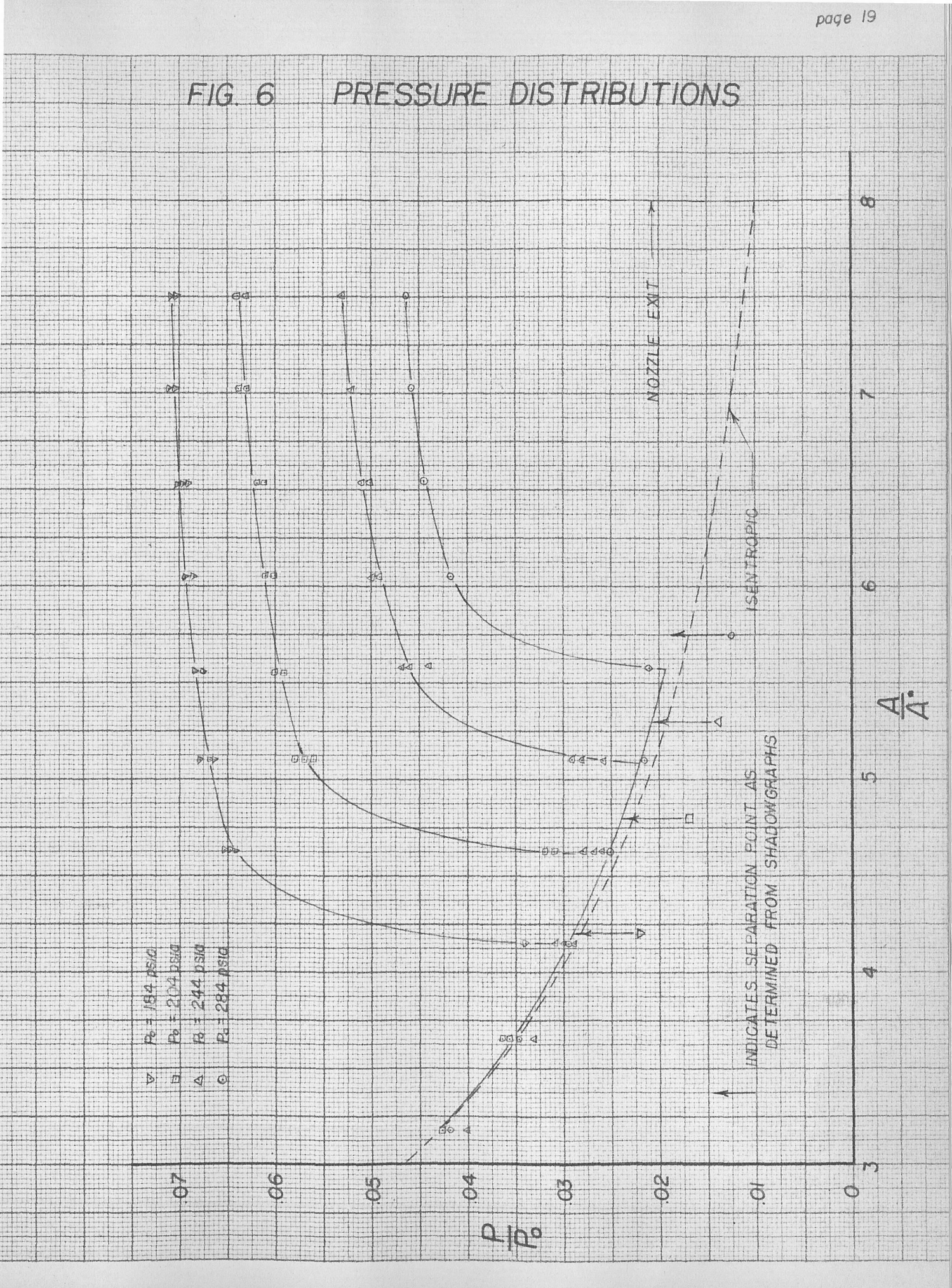

FIG. 7 PRESSURE DISTRIBUTIONS

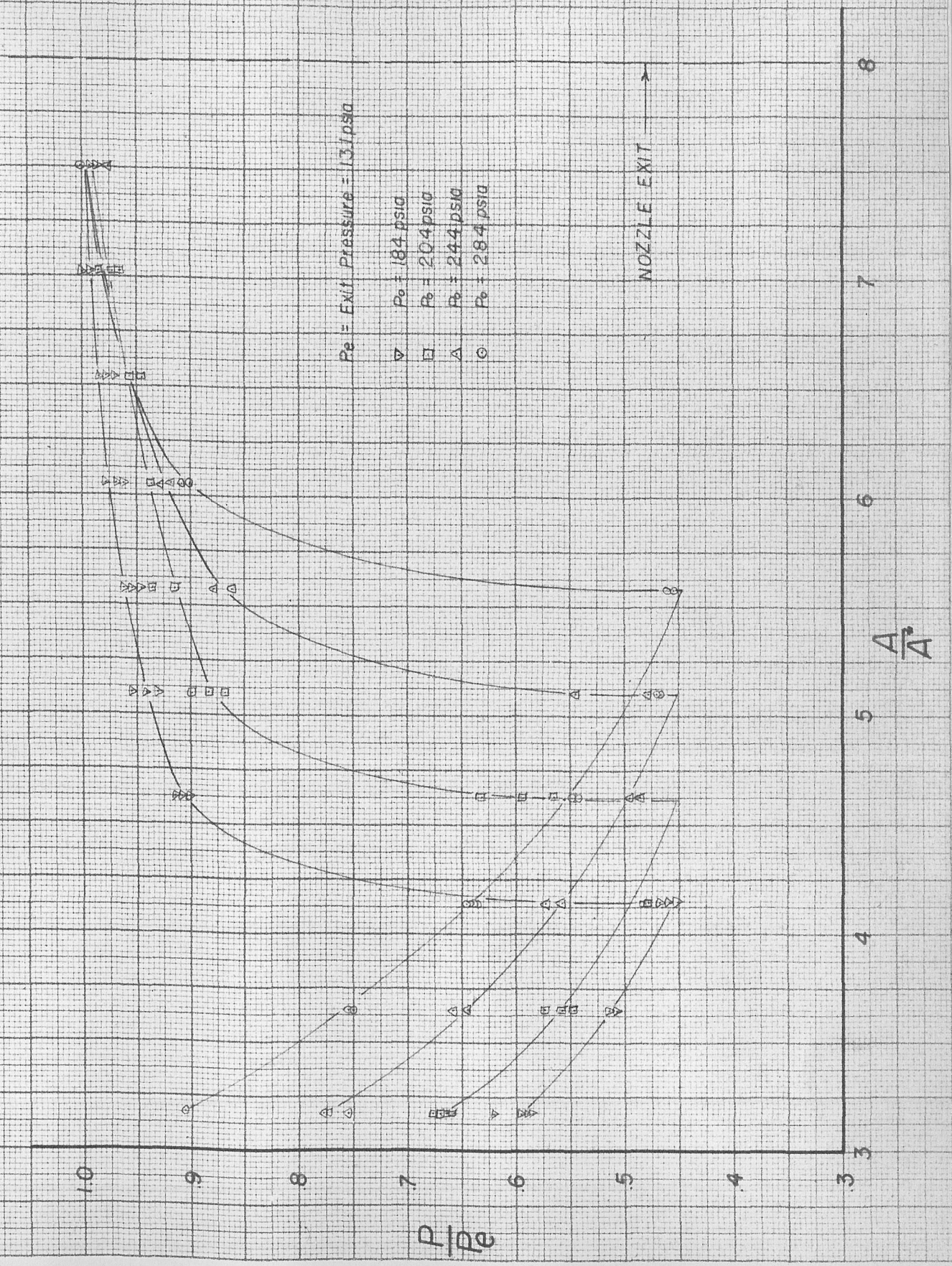

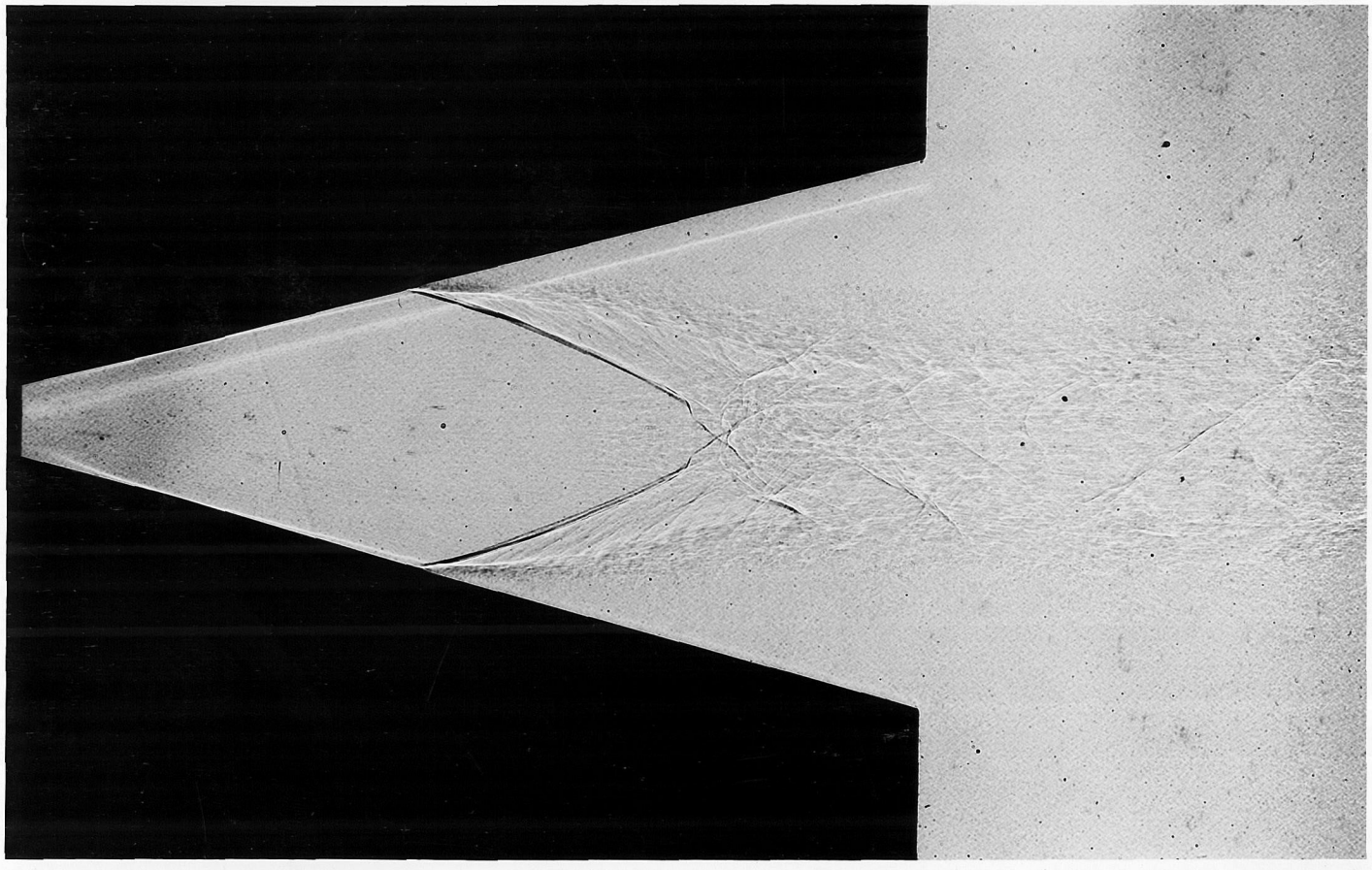

Fig. 8, $\frac{P_o}{P_e} = 12.5$

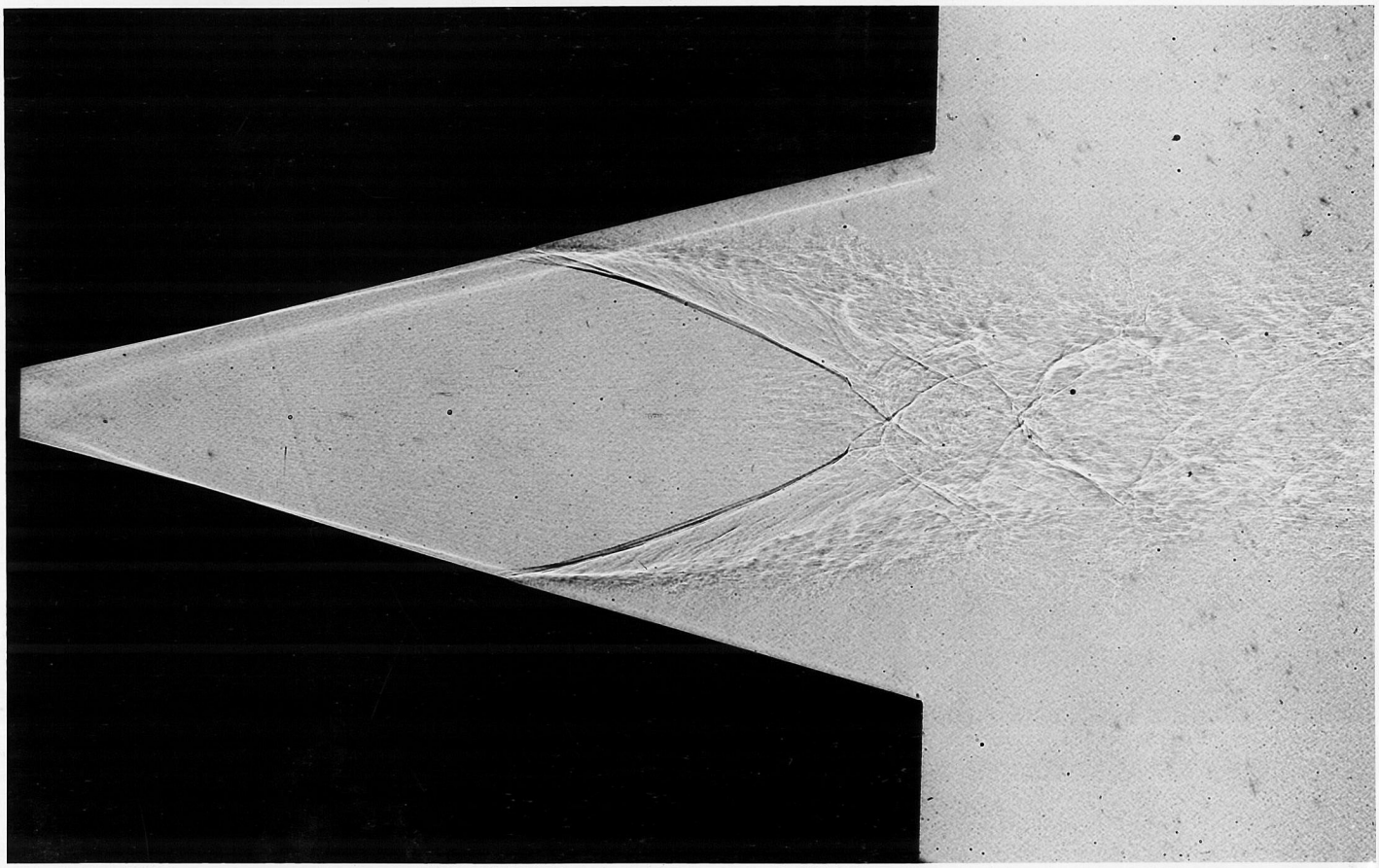

Fig. 9, $\frac{P_o}{P_e} = 15.6$

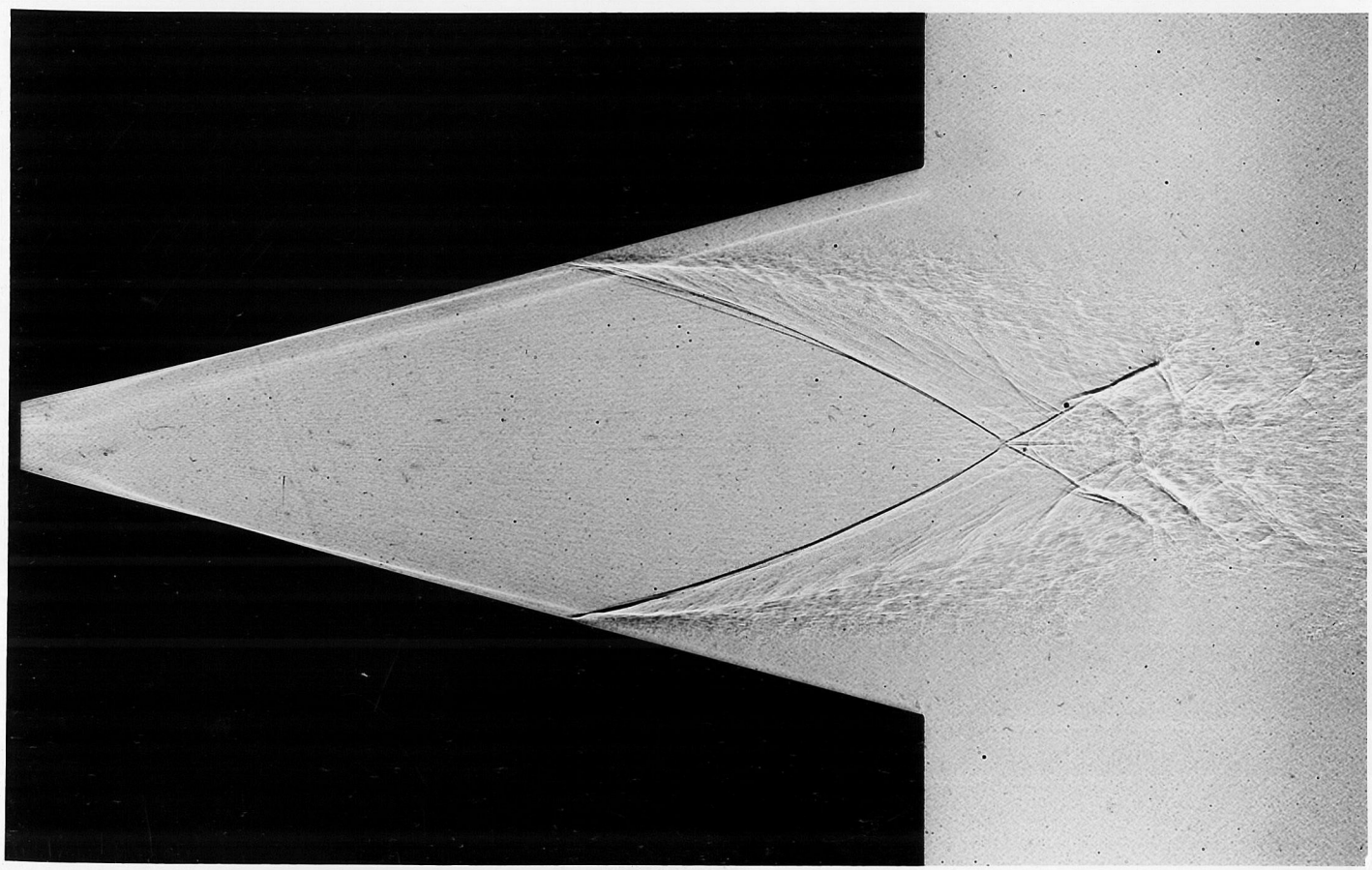

Fig. 10, $\frac{P_o}{P_e} = 19.4$

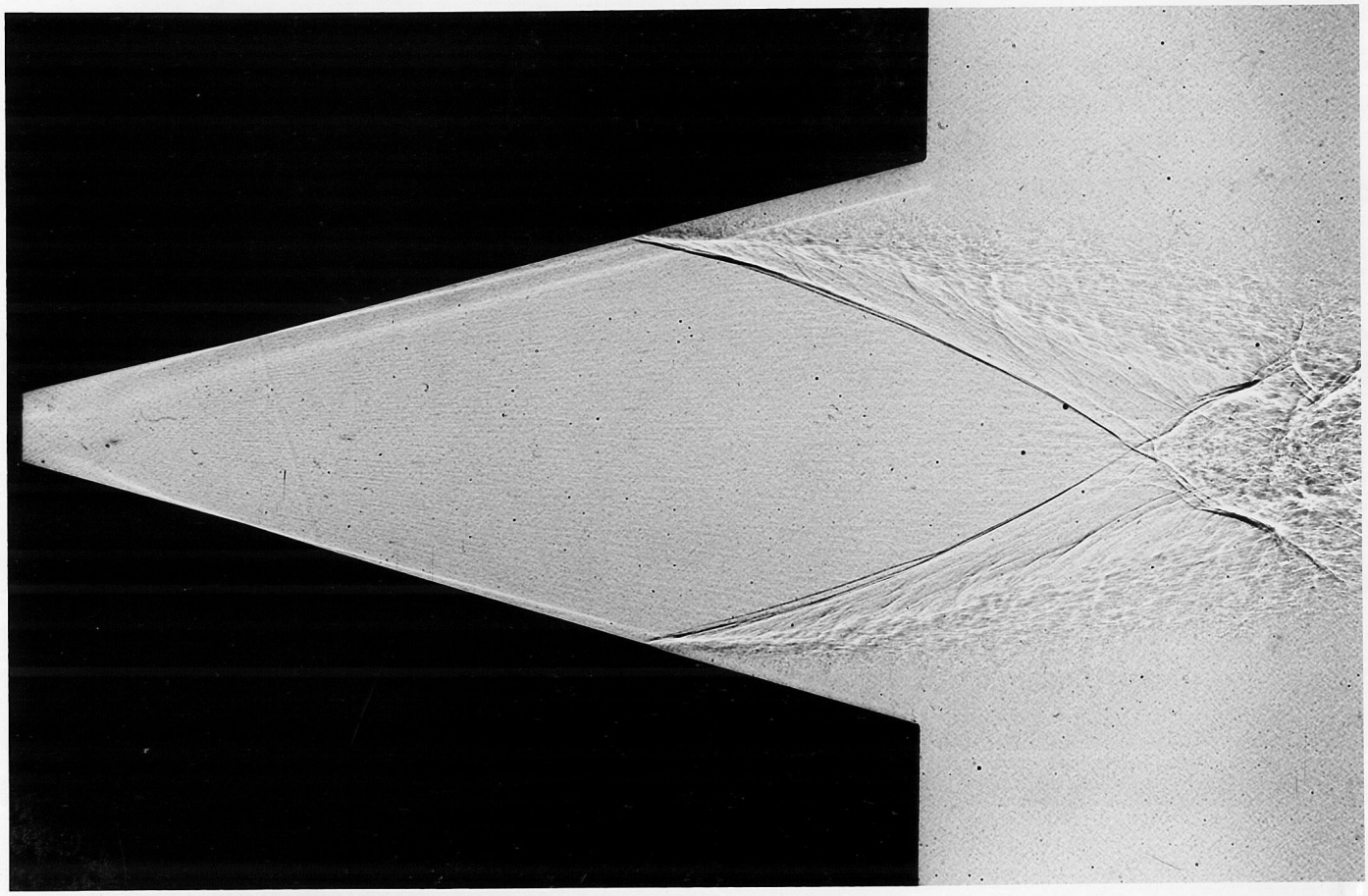

Fig. 11, $\frac{P_o}{P_e} = 21.7$

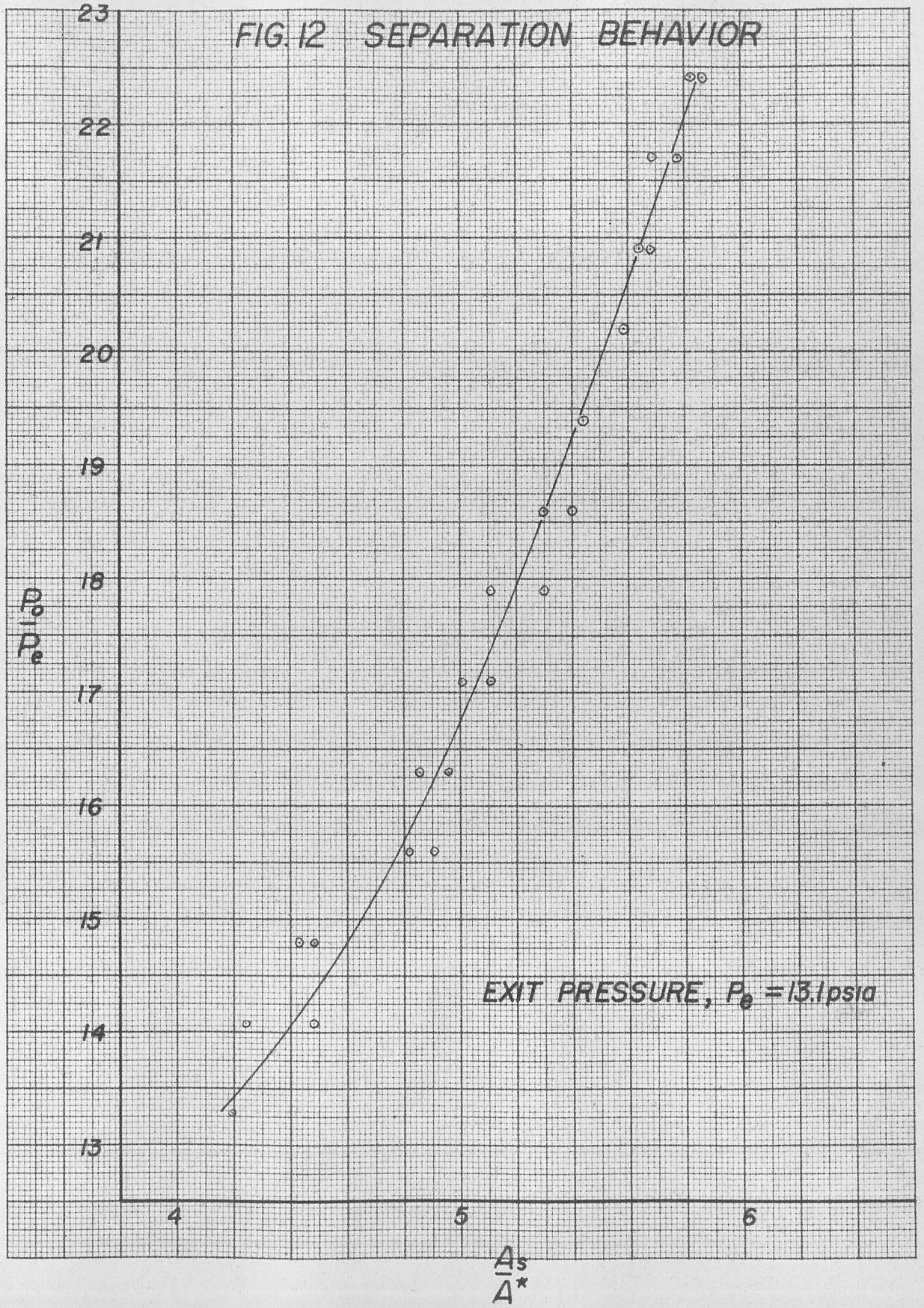
FIG. 12 SEPARATION BEHAVIOR
23
22
21
20
19
18
17
16
15
14
13
$\frac{P_o}{P_e}$
4
5
6
$\frac{A_s}{A^*}$
EXIT PRESSURE, P_e = 13.1 psia

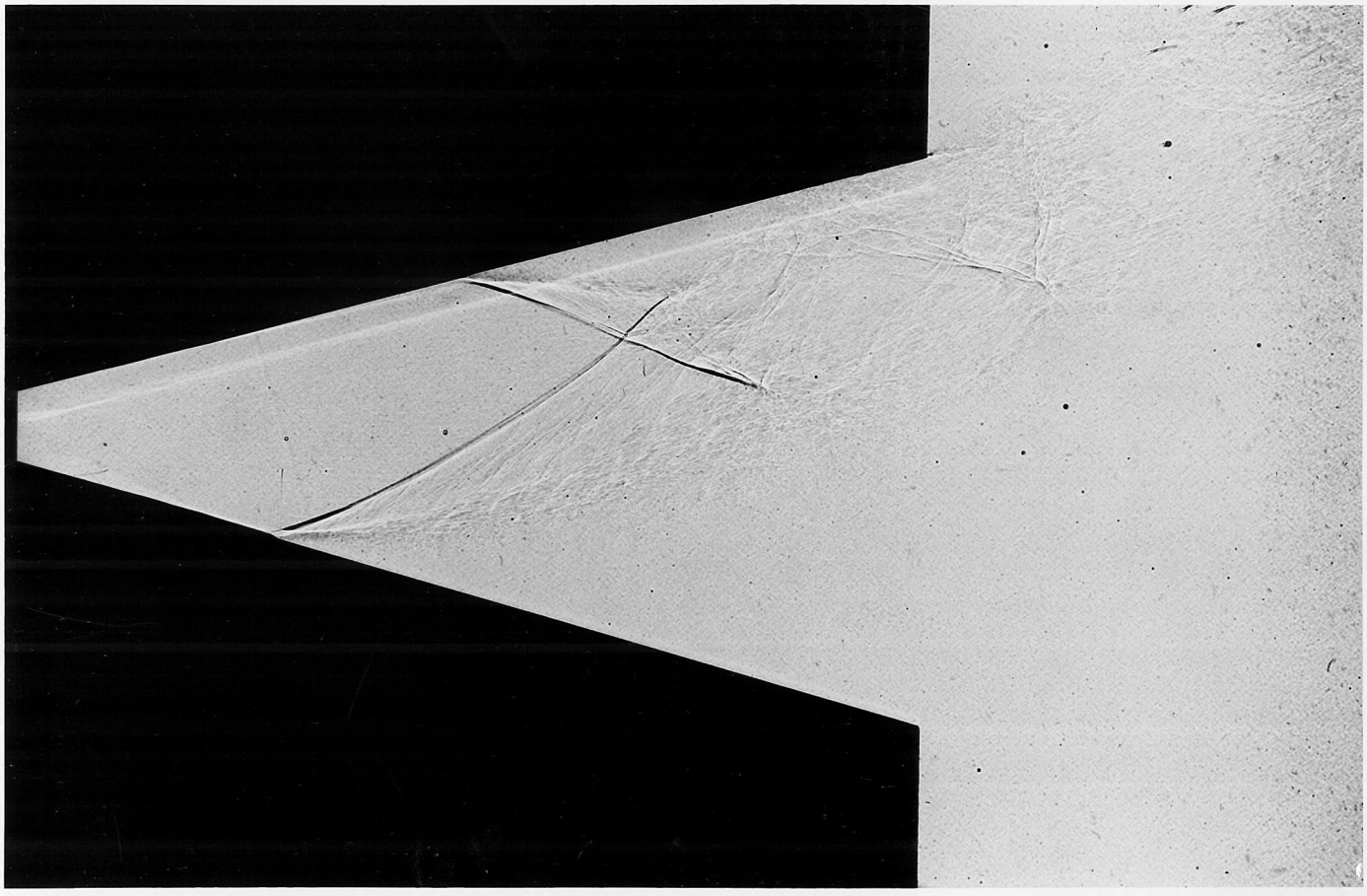

Fig. 13, $\frac{P_o}{P_e} = 8.7$

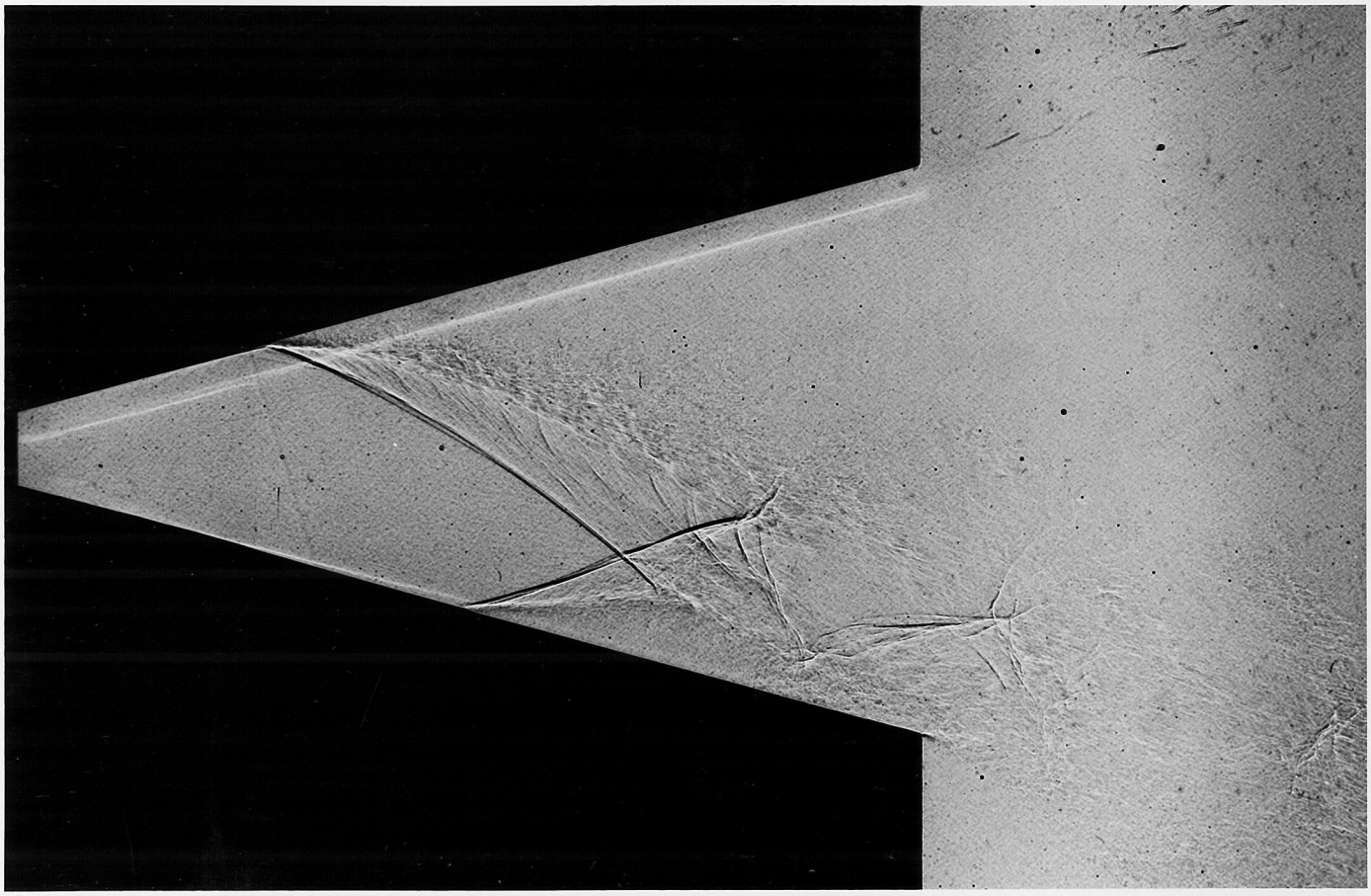

Fig. 14, $\frac{P_o}{P_e} = 8.7$

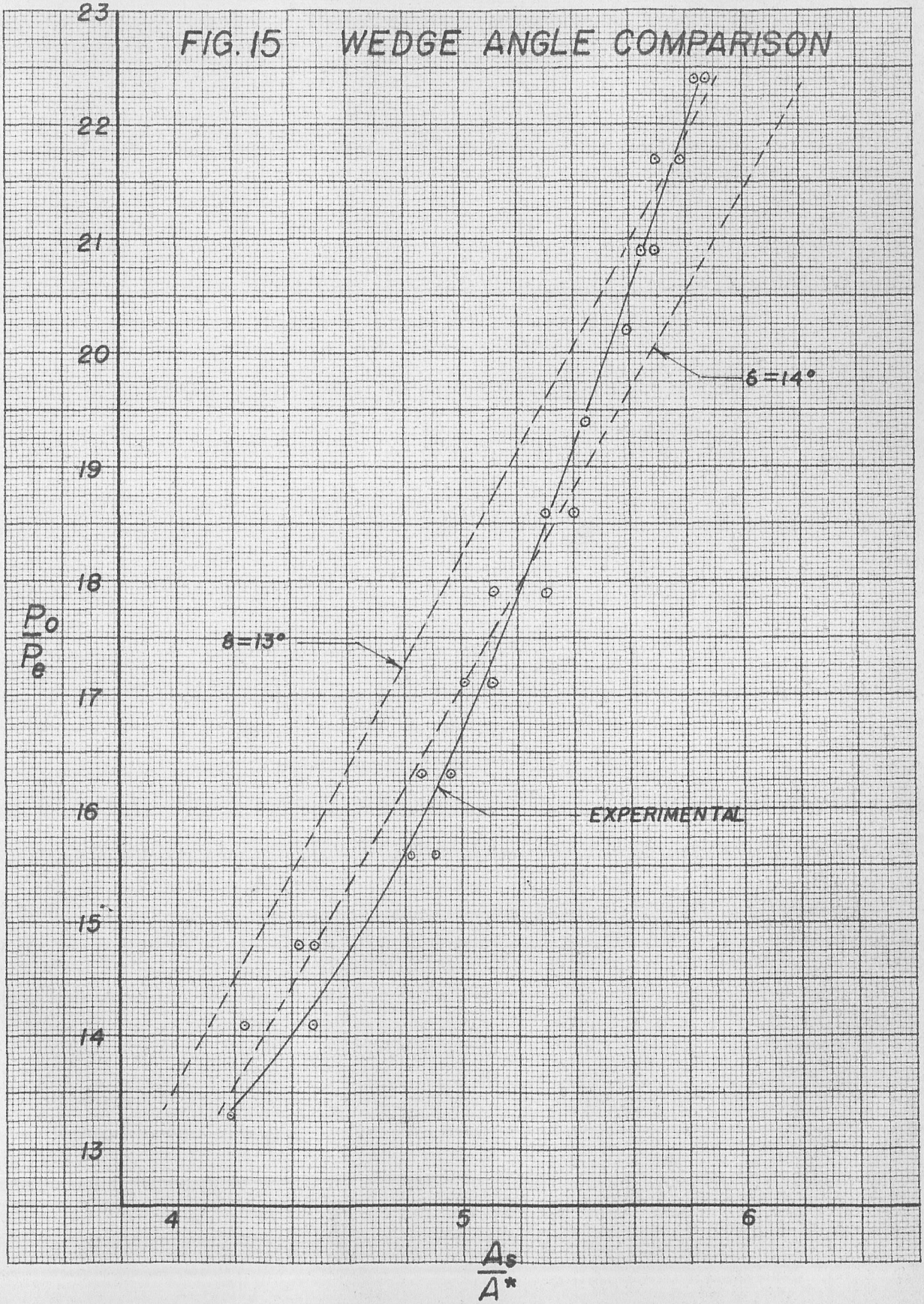
FIG. 15 WEDGE ANGLE COMPARISON
23
22
21
20
19
18
17
16
15
14
13
$\frac{P_o}{P_e}$
δ=13°
δ=14°
EXPERIMENTAL
4
5
6
$\frac{A_s}{A^*}$

FIG. 16 SEPARATION PRESSURE RATIO

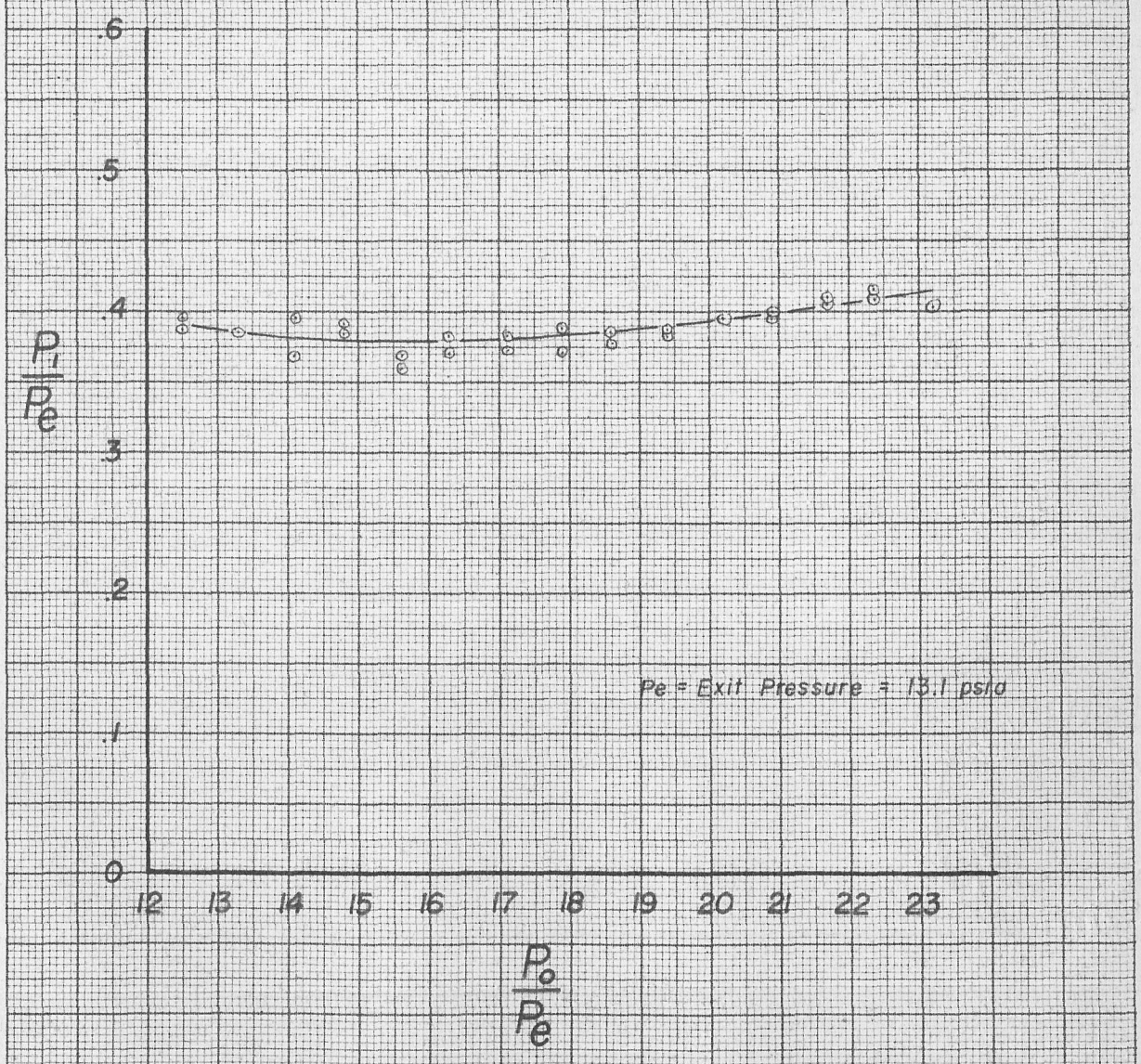

APPENDIX

I. Determination of the pressure ratio-area ratio variations for constant flow deflection as shown in Fig. 14.

The idealized flow pattern shown below is assumed to exist at the point of flow separation on the wall.

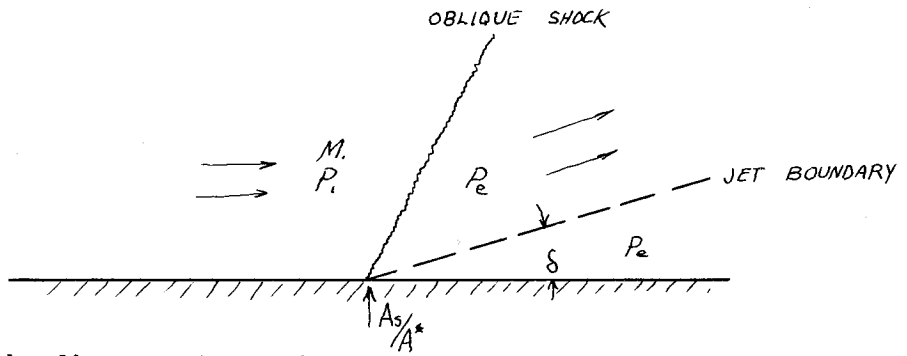

Referring to the diagram above, from the one-dimensional, isentropic nozzle theory we obtain

$$\left(\frac{A_s}{A^*}\right)^2 = \frac{1}{M_1^2}\left[\frac{2}{\gamma+1}\left(1+\frac{\gamma-1}{2}M_1^2\right)\right]^{\frac{\gamma+1}{\gamma-1}}$$

and

$$\frac{P_1}{P_0} = \left(1+\frac{\gamma-1}{2}M_1^2\right)^{\frac{\gamma-1}{\gamma}}$$

The pressure ratio P_1/P_e across the oblique shock for a given initial Mach number M, and the flow deflection δ, can be determined from an oblique shock polar diagram.

We see, then, that for an assumed value of the flow deflection and a given area ratio, we can find the corresponding pressure ratio.

The calculations for the two assumed flow deflection angles are shown in the table below.

	A /A*	M	P_e/P_1	P_1/P_o	P_o/P_e
14°	4.0	2.94	2.61	.0298	12.8
	4.5	3.06	2.70	.0249	14.9
	5.0	3.17	2.77	.0211	17.1
	5.5	3.27	2.84	.0182	19.3
	6.0	3.37	2.92	.0160	21.4
13°	4.0	2.94	2.46	.0298	13.6
	4.5	3.06	2.53	.0249	15.9
	5.0	3.17	2.60	.0211	18.2
	5.5	3.27	2.66	.0182	20.6
	6.0	3.37	2.73	.0160	22.8

II. Determination of the pressure ratio-area ratio relationship for separation at constant pressure

For one-dimensional, isentropic nozzle flow

$$\left(\frac{A_s}{A^*}\right)^2 = \frac{\gamma-1}{2} \frac{\left(\frac{2}{\gamma+1}\right)^{\frac{\gamma+1}{\gamma-1}}}{\left(\frac{P_1}{P_o}\right)^{\frac{2}{\gamma}}\left[1-\left(\frac{P_1}{P_o}\right)^{\frac{\gamma-1}{\gamma}}\right]}$$

Since we assume P_1 = constant

$$\frac{P_1}{P_o} = \frac{P_e}{P_o}\left(\frac{P_1}{P_e}\right) = k\frac{P_e}{P_o}$$

Therefore:

$$\left(\frac{A_s}{A^*}\right)^2 = \frac{\gamma-1}{2} \frac{\left(\frac{2}{\gamma+1}\right)^{\frac{\gamma+1}{\gamma-1}}}{\left(k\frac{P_e}{P_o}\right)^{\frac{2}{\gamma}}\left[1-\left(k\frac{P_e}{P_o}\right)^{\frac{\gamma-1}{\gamma}}\right]}$$